



## **Sensitivity of Mars Surface Navigation to Timing Errors**

**Todd A. Ely and David Bell**

Jet Propulsion Laboratory  
California Institute of Technology  
4800 Oak Grove Drive  
Pasadena, California, 91109

Email: [Todd.A.Ely@jpl.nasa.gov](mailto:Todd.A.Ely@jpl.nasa.gov), [David.J.Bell@jpl.nasa.gov](mailto:David.J.Bell@jpl.nasa.gov)

# **AAS/AIAA Astrodynamics Specialist Conference**

**Big Sky, Montana 3-7 August 2003**

**AAS Publications Office, P.O. Box 28130, San Diego, CA 92198**

(this page intentionally left blank)

## SENSITIVITY OF MARS SURFACE NAVIGATION TO TIMING ERRORS

Todd A. Ely<sup>\*</sup>, David Bell<sup>†</sup>

A key service of the Mars Network (MN) will be to provide Doppler tracking measurements between a Mars surface asset and a Mars Network orbiter that can be used to determine the location of the surface asset. A requirement of the Network is to provide tracking data of sufficient quality to enable position determination to better than 10 m (1-sigma) uncertainty. Numerous error sources impact the quality of this data, one of which is data time tag errors. This error manifests itself in the positioning process because the recorded time used to query orbital trajectories and the location of the surface asset in inertial space is different from the real time that the measurement was taken. This study will show that the surface asset positioning process is robust and relatively insensitive to these errors. Indeed, the combination of in-situ and MN orbiter to Earth Doppler data is capable of simultaneously resolving surface asset and MN orbiter positions to an accuracy of 10 m, and clock errors to levels better than 3 msec.

### INTRODUCTION

NASA has embarked on a detailed *in situ* investigation of Mars using landers, rovers, orbiters, and aerobots. A critical component to the success of this campaign is the development of an orbital infrastructure to support the telecommunications and navigation needs of these missions. This infrastructure, called the Mars Network (MN), will be a collection of Mars in-situ science orbiters that can also serve as relays and, eventually, a dedicated telecommunications satellite. Each of these orbiters will carry a common, reconfigurable UHF transceiver, called Electra that can transmit and receive in-situ communications and navigation data. More on MN's communication services can be found in References [1], [2], and [3]. The first element of the network will be the Mars Reconnaissance Orbiter (MRO) to be launched in 2005 and aerobrake into a 255 x 320 km altitude, Sun synchronous orbit around Mars. Its primary mission is scientific, but with Electra it can also play a critical role in establishing the first node of the network. A dedicated communications and navigation satellite, called the Mars Telesat Orbiter

---

<sup>\*</sup> Senior Engineer, Navigation and Mission Design Section, Jet Propulsion Laboratory, California Institute of Technology, MS 301-125L, 4800 Oak Grove Drive, Pasadena, CA 91109-8099. Ph: 818-393-1744, Email: [Todd.A.Ely@jpl.nasa.gov](mailto:Todd.A.Ely@jpl.nasa.gov).

<sup>†</sup> Senior Engineer, Communications Systems and Research Section, Jet Propulsion Laboratory, California Institute of Technology, MS 161-260, 4800 Oak Grove Drive, Pasadena, CA 91109-8099. Ph: 818-354-8041, Email: [David.J.Bell@jpl.nasa.gov](mailto:David.J.Bell@jpl.nasa.gov).

(MTO), is currently planned for launch in 2009 and will be put into a 4450 km altitude, circular, Sun synchronous orbit. Other elements of the network will follow. A key service that the network will provide is the formation of 2-Way Doppler tracking measurements between a Mars surface asset and a Mars Network orbiter that can be used to determine the location of the surface asset. A requirement of the network is to provide tracking data of sufficient quality to enable position determination to better than 10 m ( $1-\sigma$ ) uncertainty. Numerous error sources impact the quality of this data, one of which is Doppler data time tag errors. That is, the orbiter maintains a time reference that it uses to tag the data upon collection. The difference in time between this running clock and a standard time, such as TAI, yields a time tag error. This error manifests itself in the positioning process because the recorded time is used to query orbital trajectories and the location of the surface asset in inertial space. If this error is not properly accounted for, it can seriously impact the ability to do position determination. This paper documents analysis on the sensitivity of position determination to time tag errors and approaches for mitigating this error using estimation techniques and observation scheduling.

## TIMEKEEPING AT MARS

To set the stage for a discussion on sensitivity of surface asset positioning to time tag errors it is useful to examine the current concept for timekeeping at Mars, at least as it relates to the process envisioned for the Electra transceiver that is hosted on MRO.

If spacecraft clocks never drifted with respect to Earth-based reference clocks, such as TAI or Deep Space Network station time, they could be set once, i.e. referenced to ground clocks before launch, and all time tags derived from these spacecraft clocks would have no error relative to their reference time. Of course, in this idealized scenario there would be no issue of time tag errors affecting in-situ based navigation. In reality, spacecraft timing is based on oscillators that have random frequency fluctuations and drift and, thus, introduce timing errors. For the purposes of this study, the following model for the instantaneous frequency of an oscillator will be adopted,

$$f(t) = f_o + \Delta f + \Delta \dot{f}(t - t_o) + \frac{1}{2\pi} \dot{\Psi}(t). \quad (1)$$

where  $t$  is a uniform ‘ideal’ reference time (i.e., TAI). A perfect oscillator has a constant frequency  $f_o$ , the imperfect oscillator in Eq. (1) is distorted with additional deterministic terms representing the oscillator *syntonization* (or *frequency setability*)  $\Delta f$  (in Hz) and oscillator *aging* (or *frequency drift rate*)  $\Delta \dot{f}$  (in Hz/s) and the oscillator random phase noise process  $\Psi(t)$  (rad). A clock is derived from an oscillator by integrating its output to yield,

$$\begin{aligned}\tau(t) &= \int_{t_0}^t \frac{f(t)}{f_0} dt \\ &= t_0 + b + (1+d)(t-t_0) + a \frac{(t-t_0)^2}{2} + \frac{\Psi(t) - \Psi(t_0)}{2\pi f_0},\end{aligned}\quad (2)$$

where  $b$  is a bias offset (sec) from the initial time  $t_0$ ,  $d$  is a drift rate in sec/sec,  $a$  is an acceleration in sec/sec<sup>2</sup>. Note that,

$$d = \frac{\Delta f}{f_0}, a = \frac{\Delta \dot{f}}{f_0}. \quad (3)$$

To be able to reconstruct and predict a clock's time requires a process by which measurement pairs  $(\tau(t), t)$  of the clock time  $\tau(t)$  relative to the reference time  $t$  need to be taken, and processed to yield estimates for  $b$ ,  $d$ , and  $a$ . On Electra, the clock that time tags 2-Way Doppler data is the Electra clock (ECLK). This clock is based on a quartz crystal Ultra Stable Oscillator (USO) that has the characteristics shown Table 1. The Allan Deviation  $\sigma_A(T)$  on a  $T$  sec interval is a measure of oscillator phase noise  $\Psi(t)$  that accumulates over that interval. The Allan deviation can be used to estimate the time drift over a  $T$  sec interval from random fluctuations only (i.e., the effect of  $b$ ,  $d$ , or  $a$  are not included) using,

$$\Delta \tau = \tau(t_2) - \tau(t_1) = \sigma(t_2 - t_1)(t_2 - t_1) \quad (4)$$

For time intervals longer than tens of seconds, the frequency fluctuations of quartz oscillators typically behave like a random walk with zero mean value (i.e.,  $E[\Psi(t)] = 0$ ). This type of noise process yields the following useful relationship for relating the Allan deviation at two time intervals of interest  $T_1$  and  $T_2$ ,

$$\sigma_A(T_2) = \sigma_A(T_1) \sqrt{\frac{T_2}{T_1}}. \quad (5)$$

As an example, combining Eqs. (4), (5), and  $\sigma_A(1000\text{sec})$  from Table 1 produces an estimate of only ~14 msec time error for the ECLK after 1 year of random walk frequency fluctuations. Since ECLK's random time error is so small, once accurate estimates for  $b$ ,  $d$ , and  $a$  are obtained the error in predicting ECLK relative to TAI will be small, more on this later. The USO drives not only Electra, but is the frequency reference for some of MRO's clocks and it's Small Deep Space Transponder (SDST) which is used for DTE communications and navigation.

**Table 1: Performance Specifications for Electra’s USO**

Characteristic	Specification
Syntonzation ( $\leftrightarrow d$ )	$5 \times 10^{-8}$
Aging ( $\leftrightarrow a$ )	$5 \times 10^{-11}/\text{day}$
Allan Deviation	$\sigma_A(0.1\text{sec}) = 5.0 \times 10^{-12}$ $\sigma_A(1.0\text{sec}) = 2.5 \times 10^{-12}$ $\sigma_A(10.0\text{sec}) = 1.0 \times 10^{-12}$ $\sigma_A(100.0\text{sec}) = 2.0 \times 10^{-12}$ $\sigma_A(1000.0\text{sec}) = 2.5 \times 10^{-12}$

On MRO, determination of ECLK relative to TAI currently involves two separate clock correlations. The first is measuring ECLK relative to MRO’s spacecraft clock (SCLK). The second is measuring the correlation of SCLK with respect to TAI. This two step correlation is currently required because there is no direct method for comparing ECLK to TAI. MRO’s SCLK is actually a software clock that, for robustness in case of an oscillator failure, is a combination of several oscillators on board MRO (including Electra’s USO). Electra’s USO is used to “discipline” the SCLK so that its nominal long term stability is consistent with the USO. However, if for some reason the USO were to fail, the SCLK stability will be governed by MRO’s local oscillator, which is much less stable than the USO. Details of the SCLK design are still being investigated.

**Comparing SCLK relative to TAI**

The process of resolving the SCLK relative to TAI is assisted via NASA’s Deep Space Network (DSN) timing service. The service will collect time correlation data from MRO that will be used to estimate SCLK parameters, and could be used to estimate ECLK parameters.<sup>‡</sup> Specifically, MRO sends special purpose Time Correlation (TC) packets that include a SCLK time stamp  $\tau^{SCLK}$  of when the first bit of a reference frame synchronization marker passes a specific point in the spacecraft Earth transmission hardware. Note that:

1. A “packet” is binary data of a defined size with a binary header for identification.
2. A “frame” is a wrapper that contains packets of data plus additional information for monitoring data transmission, such as a synchronization marker which is used by the TC packet to trigger a time stamp of the SCLK.

---

<sup>‡</sup> At this time the DSN time service is used only for SCLK estimation of user deep space missions. However, ECLK parameter estimation could be added to the DSN time service catalog, or some other Mars Network entity could be created to perform this function, as well. This is a topic under consideration by the Mars Program Office at this time.

Upon reception at a Deep Space Station (DSS), this same bit in the frame synchronization marker is time stamped with the Earth Receiver Time  $t^{ERT}$  referenced to its passage through a particular point in the station hardware receive chain. Note, that for this discussion,  $t^{ERT}$  is considered to be a uniform reference time that can be related to TAI. The time stamp pairs  $(\tau^{SCLK}, t^{ERT})$  form the basis by which spacecraft clock offset and drift can be determined. Some more details of this process are:

1. During a downlink transmission, MRO generates a TC packet on a commandable interval, this could be as often as every 10 minutes.
2. The TC packet is inserted at the head of the TC frame.
3. The value of the SCLK  $\tau^{SCLK}$  is captured, placed into the TC packet and the TC frame is inserted into the downlink buffer at a known but not fixed location.
4. Knowing the number of bits ahead of the TC frame, knowing the downlink data rate, a correction factor is calculated and inserted into the TC packet.
5. As the downlink data buffer is transmitted, the TC frame is sent to Earth.
6. The TC frame is received at Earth and is stamped with the  $t^{ERT}$ .
7. The current total error budget for a single measurement of  $(\tau^{SCLK}, t^{ERT})$  between MRO and a DSS is  $\sim 20$  msec. This is primarily limited by the fact that the resolution of the spacecraft measurement system is  $1/256$  sec ( $= 7.8$  msec). A finer resolution would reduce the overall error significantly.
8. Given estimates of all the delays, including the above correction factor and other MRO delays, the 1-Way light time between MRO and the DSS, and DSS hardware delays, the DSN time service can reconstruct the time that the TC packet actually departed MRO (called the spacecraft event time or SCET). A SCET measurement  $t^{SCET}$  is related to  $t^{ERT}$  using,

$$t^{SCET} = t^{ERT} - \text{1-Way Light Time} - \text{MRO Delays} - \text{DSS Delays} . \quad (6)$$

9. Using a set of these time stamp pairs  $\{(\tau_1^{SCLK}, t_1^{ERT}), \dots, (\tau_N^{SCLK}, t_N^{ERT})\}$ , the time service can process the data using Eq. (6) to compute the time differences  $\tau^{SCLK} - t^{SCET}$  which can then be used in a time estimation algorithm to obtain estimates for the SCLK bias  $b^{SCLK}$ , drift  $d^{SCLK}$ , and acceleration  $a^{SCLK}$ .

The preceding process occurs for data that is time tagged using the SCLK. However, for this study additional time correlation data is needed between ECLK and SCLK.

### Comparing ECLK to SCLK

Associated with the SCLK is a 1 pulse per second (1pps) signal that is derived from the USO and sent to Electra. For the leading edge of each pulse, the spacecraft predicts a SCLK time stamp  $\tau^{SCLK}$  and creates an information message, "At the tone the SCLK time will be XXXX.XXX." Note that as with other spacecraft time queries this is only accurate to  $1/256$  sec. When Electra receives the 1pps signal and detects a leading edge it queries the ECLK to get a corresponding time stamp  $\tau^{ECLK}$ . Electra measures this time extremely accurately; indeed, the time error between when the edge passes the detection

hardware and when Electra gets an ECLK reading is 60 nanoseconds and records it with  $\sim 60$  nsec resolution. (This may increase to 90 nsec, upcoming tests of Electra will determine the actual levels.) This is also the same accuracy that Electra is able to time tag its Doppler data. Electra then forms telemetry data of these time stamp pairs  $\{(\tau_1^{ECLK}, \tau_1^{SCLK}), \dots, (\tau_N^{ECLK}, \tau_N^{SCLK})\}$  that is sent to Earth for processing. Clearly, the 20 msec error associated with the SCLK correlation process is the more significant error source in the end-to-end time correlation problem. Recall that the SCLK is ‘disciplined’ by the USO, and frequency source for the 1pps and the ECLK is also the USO, thus the drift characteristics of the SCLK, 1pps, and ECLK should be the same. There will most likely be bias offsets between them, but, they will drift with the same rate and in the same direction. This implies that processing data sets of  $\{(\tau_1^{ECLK}, \tau_1^{SCLK}), \dots, (\tau_N^{ECLK}, \tau_N^{SCLK})\}$  to resolve the ECLK time with respect to SCLK time results in a value for a bias time offset between the two clocks (and no relative drift or acceleration), that is,

$$\begin{aligned} b^{ECLK} &= b^{ECLK-SCLK} + b^{SCLK} \\ d^{ECLK} &= d^{SCLK} \\ a^{ECLK} &= a^{SCLK} \end{aligned} \tag{7}$$

A crucial observation can be made about the preceding discussion, the ECLK is an independent free running clock with a small random drift rate that is governed by the USO, and has a clock query mechanism that is extremely accurate. This implies that if the bias offset between ECLK and TAI can be determined, then Electra Doppler time tags will be very accurate (after calibration) and have a very small random component (i.e.,  $\sim 60$  nsec). The fact that querying the SCLK is noisy (with a 20 msec uncertainty) is independent of the Doppler time tags. Now, the SCLK (and, by implication the ECLK) drift can be observed via several processes:

1. Using  $\{(\tau_1^{ECLK}, \tau_1^{SCLK}), \dots, (\tau_N^{ECLK}, \tau_N^{SCLK})\}$  and  $\{(\tau_1^{SCLK}, t_1^{ERT}), \dots, (\tau_N^{SCLK}, t_N^{ERT})\}$  data set, the DSN time service can estimate the SCLK and ECLK parameters. It is anticipated that this service can produce estimates of clock bias offsets that are accurate to a least 10 msec, and estimates of clock drift that are accurate to within  $\sim 1 \times 10^{-10}$ .
2. Using 1-Way DTE Doppler between MRO and a DSN station, the MRO navigation process can determine the USO frequency syntonization error and aging, which, because of the relationships in Eq. (3), leads to the ECLK drift and acceleration. This approach is possible because the USO drives the SDST which transmits the carrier signal to the DSN for collecting 1-Way Doppler data. It is anticipated that this approach could produce estimates of a clock drift that are accurate to  $\sim 3 \times 10^{-13}$ , however this process may not be available as often as the first method.

Given these very accurate estimates for clock drift, the central question that this paper addresses is the sensitivity of surface asset positioning using 2-Way in-situ Doppler data

with time tags that might have a biased error of 10 msec, 20 msec, or larger relative to TAI. Observability of and sensitivity to clock drift errors will be examined as well.

## **SURFACE ASSET POSITIONING**

The Mars Network will accomplish position determination of surface assets on Mars using either 1-Way or 2-Way coherent Doppler data from the proximity link. Electra actually collects total count carrier phase data  $\phi(\cdot)$  that can be processed to form a Doppler measurement  $F(\cdot)$ , using,

$$F(t_e) \equiv -\frac{\phi(t_e) - \phi(t_s)}{2\pi T} \text{ (Hz)}, \quad (8)$$

where time  $t$  is the ‘true’ (but not known) time and the Doppler data value is collected over a “count” interval  $T = t_e - t_s$  (“e” = end, “s” = start). In the 1-Way mode, one end of the link transmits and the other end tracks the received signal and collects carrier phase data. Use of 2-Way data implies that one end of the link is using Electra as a coherent transponder— typically the surface asset, and the other end of link transmits the signal and collects the data on the signals return. 2-Way data is the more accurate of the two types because it is formulated to minimize the impact of oscillator instabilities. Because of its inherent accuracy, 2-Way Doppler is the standard data type used by the MN for surface asset positioning. This in-situ data can be augmented with direct-to-Earth (DTE) Doppler and range data taken by the Deep Space Network (DSN) to any of the assets (surface or MN orbiter) with a DTE capability. The combination of the proximity data and the DTE data provides good observation geometry such that it is possible to achieve position accuracies of 10 m (1- $\sigma$ ) or less. In the ensuing analysis the affect of in-situ 2-Way Doppler time tag errors at achieving the 10 m accuracy goal is investigated.

## **IMPACT OF TIMETAG ERRORS ON ELECTRA DOPPLER DATA**

This analysis uses a differenced range formulation, pioneered by Moyer [4] for use by the DSN in the late 60’s, and has been adapted by Ely [5] for processing Electra 2-Way Doppler data in the positioning filter. Specifically, a 2-Way Doppler measurement  $F_2(t_e)$  taken at time  $t_e$  can be shown equal to the following relationship,

$$\begin{aligned}
F_2(t_e) &= M_T (f_o + \Delta f) \frac{LT(t_e) - LT(t_s)}{T} + \dots \\
&\quad \frac{M_T \Delta \dot{f}}{T} \left[ (t_e - t_{e_o})(LT(t_e) - LT(t_{e_o})) - (t_s - t_{s_o})(LT(t_s) - LT(t_{s_o})) + \text{H.O.T.} \right] + \nu(t_e) \\
&= M_T f_o \left\{ \begin{aligned} &(1+d) \frac{LT(t_e) - LT(t_s)}{T} + \dots \\ &\frac{a}{T} \left[ (t_e - t_{e_o})(LT(t_e) - LT(t_{e_o})) - (t_s - t_{s_o})(LT(t_s) - LT(t_{s_o})) + \text{H.O.T.} \right] \end{aligned} \right\} + \nu(t_e)
\end{aligned} \tag{9}$$

where the following applies:

1. The frequency terms  $f_o$ ,  $\Delta f$ ,  $\Delta \dot{f}$  conform to the model given in Eq. (1), except that the USO output frequency has been multiplied up to the nominal UHF transmission frequency ( $f_o \sim 440$  MHz).  $M_T$  is the turnaround ratio at the transponder so that the nominal receive frequency is  $M_T f_o \sim 400$  MHz.
2. The subscript 'o' refers to the epoch time that is associated with the values used for the frequency terms.
3.  $LT(t)$  is the round trip light time between the MN orbiter and surface asset. For this study the approximation,

$$LT(t) \approx \frac{2}{c} \rho(t) = \frac{2}{c} \sqrt{\boldsymbol{\rho}(t) \cdot \boldsymbol{\rho}(t)} = \frac{2}{c} \sqrt{(\mathbf{r}^{sc}(t) - \mathbf{r}^{sa}(t)) \cdot (\mathbf{r}^{sc}(t) - \mathbf{r}^{sa}(t))} \tag{10}$$

is used, where  $\rho(t)$  and  $\boldsymbol{\rho}(t)$  are the slant range and slant range vector between the spacecraft and the surface asset, respectively;  $\mathbf{r}^{sc}(t)$  is the position vector of the MN spacecraft; and  $\mathbf{r}^{sa}(t)$  is the position vector of the surface asset.

4. H.O.T. refers to neglected higher order terms.
5. The Mars Network operating with Electra transceivers has been designed such that 2-Way Doppler measurements have a very small noise  $\nu(t)$  component. Nominally, this noise is zero mean with a standard deviation of 0.27 mHz (or, equivalently, 0.1 mm/sec range rate error) on a 20 sec count interval.<sup>5</sup>
6. Finally, the last equality in Eq. (9) follows from the fact that the USO drives both the Electra carrier signal and the ECLK (modeled using Eq. (2)), thus, the clock drift  $d$  and acceleration  $a$  have replaced the syntonization  $\Delta f$  and aging  $\Delta \dot{f}$  terms of the oscillator.

Equation (9) is a model for the actual Doppler shift that is measured by Electra (using carrier phase) at the 'true' time  $t_e$  at the end of the count interval, however this time is

not known in operations. In fact, when Electra measures a carrier phase  $\phi(t_e)$  value it queries the ECLK and time tags the phase measurement with the time  $\tau(t_e) \equiv \tau^{ECLK}(t_e)$  (where for notational simplicity the superscript ECLK has been dropped). Electra collects a set of carrier phase data and associated time tags  $\{(\phi(t_{e,1}), \tau(t_{e,1})), \dots, (\phi(t_{e,N}), \tau(t_{e,N}))\}$  that is, nominally, transmitted back to Earth. Before processing the carrier phase data to get Doppler, the ECLK time tags are calibrated using the current nominal model for ECLK using,

$$\begin{aligned} \tau^c(t) &= \tau(t) - \left( \bar{b} + \bar{d}(t-t_o) + \bar{a} \frac{(t-t_o)^2}{2} \right) \\ &= (\hat{b} - \bar{b}) + (\hat{d} - \bar{d} + 1)(t-t_o) + (\hat{a} - \bar{a}) \frac{(t-t_o)^2}{2} + \frac{\Psi(t) - \Psi(t_o)}{2\pi f_o}, \quad (11) \\ &\equiv \Delta b + (\Delta d + 1)(t-t_o) + \Delta a \frac{(t-t_o)^2}{2} + \frac{\Psi(t) - \Psi(t_o)}{2\pi f_o} \end{aligned}$$

where the carat '^' refers to actual values (which, in operations, are not known in the case of the real ECLK) and the over bar '^-' refers nominal values (which are known). The calibrated ECLK values  $\tau^c(t)$  have an associated model for the bias  $\Delta b$  and drift  $\Delta d$  that are currently unknown and, later, will be solved for by the filter. Using the computed  $\tau^c(t)$  the carrier phase values at the start and end of a count interval are converted into a Doppler measurement using Eq. (8) as follows,

$$\hat{F}_2(t_e) \equiv -\frac{\phi(t_e) - \phi(t_s)}{2\pi(\tau_e^c - \tau_s^c)} \quad (12)$$

note, that for notational simplicity  $\tau_e^c \equiv \tau^c(t_e)$  and  $\tau_s^c \equiv \tau^c(t_s)$ , and the carat '^' refers to the fact that this is an recorded measurement. This data can then be used by a filter to determine the position of the surface asset. In order to actually do this, the filter formulates a computed measurement using nominal models for the MN orbiter trajectory, the surface asset location, and the calibrated time tag of the data using,

$$\bar{F}_2(t_e) \equiv \frac{2M_T \bar{f}_o}{c} \left( \frac{\bar{\rho}(\tau_e^c) - \bar{\rho}(\tau_s^c)}{\tau_e^c - \tau_s^c} \right) \quad (13)$$

where the bar '^-' indicates that all the quantities are computed using nominal values. Now to determine the sensitivity of the measurement to time tag errors, difference Eq. (13) from Eq. (12) and expand using a Taylor series around the nominal values for the clock bias  $\bar{b}$  and drift  $\bar{d}$ . For now ignore other errors, such as surface asset position errors. The result is as follows,

$$\delta F_2 = \hat{F}_2(t_e) - \bar{F}(\tau_e^c) = \left. \frac{\partial \bar{F}_2(\tau_e^c)}{\partial b} \right|_{\tau_e^c, \tau_s^c} (0 - \delta b) + \left. \frac{\partial \bar{F}_2(\tau_e^c)}{\partial d} \right|_{\tau_e^c, \tau_s^c} (0 - \delta d) + \text{H.O.T.} \quad (14)$$

where the value 0 appears in  $(0 - \delta b)$  and  $(0 - \delta d)$  because an ideal clock has no bias or drift. Eq. (14) represents that portion of a measured Doppler shift measurement this is due to errors in modeling the ECLK. The partials in Eq. (14) take the form,

$$-\left. \frac{\partial \bar{F}_2(\tau_e^c)}{\partial b} \right|_{\tau_e^c, \tau_s^c} = -\frac{2M_T \bar{f}_o}{c} \frac{1 + \bar{d}}{\tau_e^c - \tau_s^c} \left( \frac{d\bar{\rho}(\tau_e^c)}{dt} - \frac{d\bar{\rho}(\tau_s^c)}{dt} \right) \quad (15)$$

and,

$$-\left. \frac{\partial \bar{F}_2(\tau_e^c)}{\partial d} \right|_{\tau_e^c, \tau_s^c} = -\frac{2M_T \bar{f}_o}{c} \left\{ \frac{1}{\tau_e^c - \tau_s^c} [\bar{\rho}(\tau_e^c) - \bar{\rho}(\tau_s^c)] + \dots \right. \\ \left. \frac{1 + \bar{d}}{\tau_e^c - \tau_s^c} \left[ (\tau_e^c - \tau_{e_0}^c) \frac{d\bar{\rho}(\tau_e^c)}{dt} - (\tau_s^c - \tau_{s_0}^c) \frac{d\bar{\rho}(\tau_s^c)}{dt} \right] \right\} \quad (16)$$

It is illustrative to compare the Doppler signature of these errors relative to a 10 m surface asset position error. Consider a pass between MRO and a surface asset. A 10 m position error, a 1 msec clock bias error, a  $5 \times 10^{-10}$  clock drift rate error, and a 60 nsec random clock query error are all shown in Figure 1. The clock bias error of 1 msec is of the same order as a 10 m position error (20 mm/sec versus 60 mm/sec magnitude). The drift and random clock errors are significantly less than 0.1 mm/sec (the expected Doppler noise level). Hence, it is anticipated that the navigation filter should be readily able to resolve a clock bias error, however a clock drift rate error will be much more difficult to determine. The ability of a navigation filter to simultaneously estimate surface asset position components, MN orbiter trajectory initial conditions, and clock components using in-situ Doppler data and/or DTE Doppler data is examined in the next section.

## SURFACE ASSET POSITIONING WITH TIME TAG ERRORS

In this section simulation results for various scenarios involving Electra 2-Way Doppler time tag errors are presented. The analysis assumes a simplified scenario, where the only error sources are clock errors, data noise, and initial condition errors for the surface asset and the MN orbiter. Using these error models, a recursive, UDU-factorized Kalman filter can be constructed that estimates corrections to the nominal values for the fixed position states of the surface asset, clock bias and drift parameters, and orbiter initial conditions. In order to isolate the effect of the time tag error, all other error sources (multipath effects, atmospheric delays, etc.) are ignored. The recursive filter has been formulated to estimate for errors in the initial state (i.e., it is an 'epoch' state filter). This error vector is represented formally as,

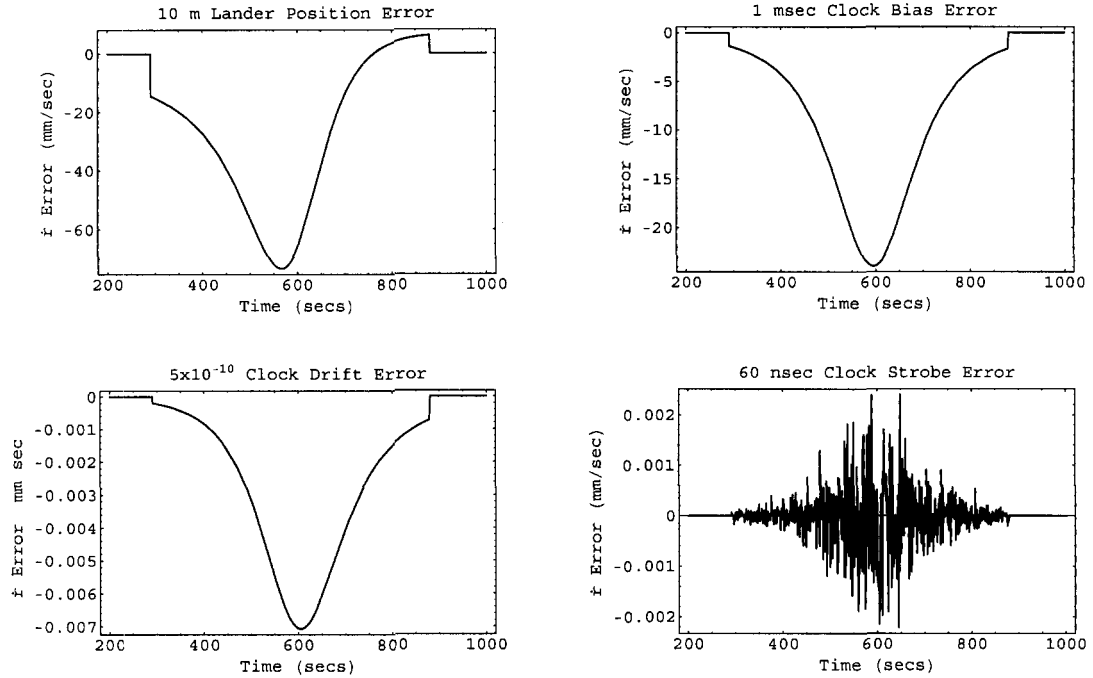


**Figure 1:** Doppler shift (expressed as an equivalent range rate) due to a surface asset position error and clock model errors.

$$\delta \mathbf{x}(t_o) = \hat{\mathbf{x}}(t_o) - \bar{\mathbf{x}}(t_o) \quad (17)$$

where, as before, the carat refers to the actual values and the bar refers to the nominal values. The components of the filter state vector are defined to be  $\mathbf{x}(t_o) = \{x_o^{sa}, y_o^{sa}, z_o^{sa}, \delta b, \delta d, a, e, i, \Omega, \omega, M_o\}$ , which includes the initial position components of the surface asset in inertial Cartesian coordinates  $\{x_o^{sa}, y_o^{sa}, z_o^{sa}\}$ , the clock bias  $\delta b$  and drift rate  $\delta d$ , and the initial classical elements  $\{a, e, i, \Omega, \omega, M_o\}$  of the MN orbiter. The epoch state model that the filter operates on conforms to,

$$\delta \mathbf{x}(t) = \delta \mathbf{x}(t_o) + \mathbf{n}(t), \quad (18)$$

where the process noise term  $\mathbf{n}(t)$  is small, and is used primarily for tuning the filter and to keep it numerically well behaved. The measurement model for the filter takes the form,

$$\delta F_2(t) = \hat{F}_2(t) - \bar{F}_2(t) = \frac{\partial F_2(t)}{\partial \mathbf{x}(t_o)} \delta \mathbf{x}(t_o) + \nu(t) = \mathbf{h}^\top(t) \delta \mathbf{x}(t_o) + \nu(t), \quad (19)$$

where the partials with respect to the surface asset initial conditions and the orbiter classical elements are standard, and won't be repeated here. The partials with respect to

the clock parameters are given by Eqs. (15) and (16) (including the preceding ‘–’ shown). A UDU formulation for the Kalman filter is found in Bierman [6]. At each forward step in time  $t_n$  the filter outputs estimates of the initial state error  $\widehat{\delta\mathbf{x}}(t_n)$ , and its associated covariance  $\mathbf{P}(t_n)$ . It should be noted that the time increments correspond to measurement times  $t_n$ . Hence, the time increment is uneven; that is, during a measurement gap  $t_n - t_{n-1}$  can be many hours in length, and during a tracking pass  $t_n - t_{n-1}$  is nominally 20 secs. The process noise covariance  $E[\mathbf{n}(t)\mathbf{n}^\top(t)] = \mathbf{Q}(t_n)$  takes the form,

$$\mathbf{Q}(t_n) = \text{diag} \left\{ \sigma_x^2, \sigma_y^2, \sigma_z^2, \sigma_{wp}^2, \frac{\sigma_A^2(T_A)}{T_A}(t_n - t_{n-1}), \sigma_a^2, \sigma_e^2, \sigma_i^2, \sigma_\Omega^2, \sigma_\omega^2, \sigma_{M_o}^2 \right\}. \quad (20)$$

where the driving noise levels are scenario dependent (but typically several orders of magnitude less than the actual error). Since this is a simulation the true values of all parameters are known, hence it is possible to form the filter error vector  $\mathbf{e}(t_n) \equiv \delta\mathbf{x}(t_n) - \widehat{\delta\mathbf{x}}(t_n)$  (by implication, this is the error in the estimate of the initial error) and then compare components of this vector to their associated 1-sigma values from the covariance (i.e.,  $|e_i(t_n)| < \sqrt{P_{ii}(t_n)}$ ), or the root sum square (RSS) of selected components. A properly tuned and operating filter should exhibit error magnitudes that are smaller than their associated 1-sigma uncertainties.

Finally, the errors in the estimate for the clock are shown in current time, and can be constructed from  $\widehat{\delta\mathbf{x}}(t_n)$  using,

$$|\tilde{\tau}_n - \tau_n| = \left| \begin{aligned} & \left( (\bar{b} + \delta\tilde{b}_n) + (\bar{d} + \delta\tilde{d}_n)(t_n - t_o) + \bar{a} \frac{(t_n - t_o)^2}{2} - \dots \right) \\ & \left( \hat{b} + \hat{d}(t_n - t_o) + \hat{a} \frac{(t_n - t_o)^2}{2} + \frac{\psi(t_n) - \psi(t_o)}{2\pi\hat{f}_o} \right) \end{aligned} \right| \quad (21)$$

An associated uncertainty can be formed from Eq. (21) by computing  $E[(\tilde{\tau}_n - \tau_n)^2]$ . Similarly, orbiter trajectory errors at  $t_n$  are shown by mapping the initial conditions and uncertainties forward from  $t_o$  to  $t_n$ .

## SIMULATION RESULTS

The assumptions and simulation parameters that that are common to all the simulations are as follows:

1. The surface asset is located on the equator and has a  $15^\circ$  minimum elevation angle.
2. The simulated surface asset position error is 1 km in X, Y, and Z.
3. The MN orbiter is typically MRO in a 320x255 km, Sun-synchronous orbit. The nominal orbiter differs in initial position from the actual one by  $\sim 50$  m. This is consistent with current operational experience with science orbiters at Mars. A case with MTO in a 4450x4450 km altitude, Sun-synchronous is also examined.
4. Cases with DTE data consists of Doppler data between the MN orbiter and, typically, the station at Madrid (DSS 45). No DTE data to the surface asset is used. Since the DTE data is time tagged at Earth, there is no sensitivity to ECLK clock errors. Hence, the DTE data can only be used to estimate the orbiter trajectory.
5. The ‘true’ ECLK is simulated with a 50 msec bias offset, a  $5 \times 10^{-8}$  drift rate, an oscillator random walk frequency drift with Allan deviation of  $10^{-12}$  on a 60 sec count, and a clock query noise of 60 nsecs. Note that the clock acceleration is present, but has negligible impact on all the simulated results. The ‘nominal’ ECLK will vary depending on the scenario.
6. The filter initial condition is the zero vector  $\delta \mathbf{x}(t_o) = \mathbf{0}$ ,
7. The filter initial covariance is diagonal with each element set to  $(100 \times \delta x_i(t_o))^2$  where  $\delta x_i(t_o)$  is the initial condition error for component  $i$ .
8. Finally, the simulation length is 100 hrs.

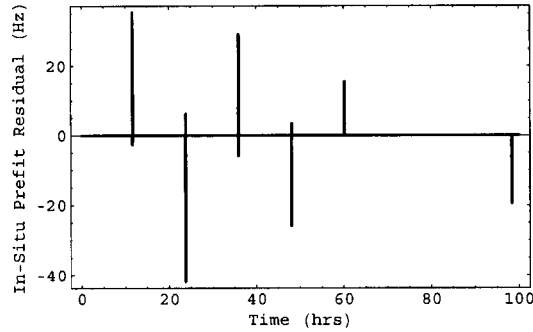
An example of the Doppler shift (in Hz) induced by the aforementioned initial condition errors between a surface asset at the equator and MRO is illustrated in Figure 2. The shift represents the pre-fit residual that is passed to the filter for estimation. Note that the tracking passes between the surface asset and MRO are typically 5 to 7 minutes in length and occur very infrequently for a lander at the equator. A typical period between passes is on the order of 12 hrs, but can last for days. Because of MTO’s higher altitude orbit, the average pass is much longer, about 1 hour, and the average gap between passes is about 6 hrs, with the longest being  $\sim 16$  hrs. Also shown in the figure are the tracking passes between MRO and DSS 45. These passes occur once a day and last about 8 – 10 hrs.

### Case 1

This example represents a basis for comparison, and has the following details:

1. It has in-situ Doppler data only between the surface asset and MRO. There is no DTE data.
2. There is no time tag error, that is  $\tau = t$ . The only errors are surface asset and MRO initial condition errors and data noise.

### In-Situ Link between MRO and Surface Asset



### DTE link between MRO and DSS 45

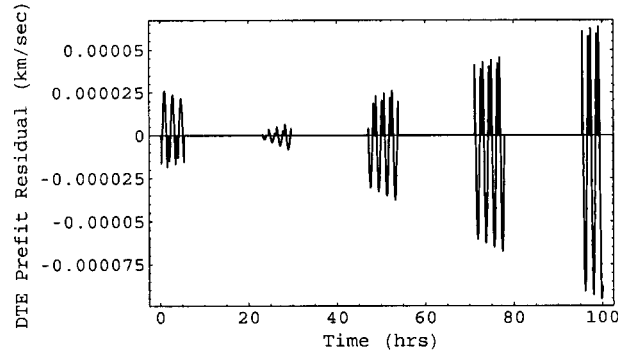


**Figure 2:** Error in the Doppler shift due to the orbiter, surface asset, and clock errors prior to filter (i.e., pre-fit residuals).

3. The filter estimates for the surface asset and the orbiter initial conditions, however it does not estimate for any clock components.
4. The process noise  $\mathbf{Q}(t)$  has been set to very small levels, about  $1/10000^{\text{th}}$  of the actual errors. With process noise this small the filter essentially becomes a recursive weighted least squares filter, however the noise is sufficient to keep the filter solution stable.

The results for the magnitude of the surface asset position error and the magnitude of the orbiter trajectory error are shown in Figure 3. The solid lines in both figures represent the RSS difference between the filter solution and the known initial condition corrections. The dashed line is the associated 1-sigma uncertainty associated with the RSS error, and is obtained from the covariance output of the filter. For both the surface asset and orbiter the filter is well behaved by producing solutions with errors that are consistent with the statistics. Note that both the surface asset and the orbiter have approximately an 8m 1-sigma uncertainty after about 3 passes of data. The 8-m level exists because the surface asset's Y-coordinate  $y^{sa}$  and the orbiter's right ascension of the ascending node  $\Omega$  are fully correlated ( $P_{y^{sa}, \Omega} / (\sigma_{y^{sa}} \sigma_{\Omega}) = -0.99$ ). Examination of the

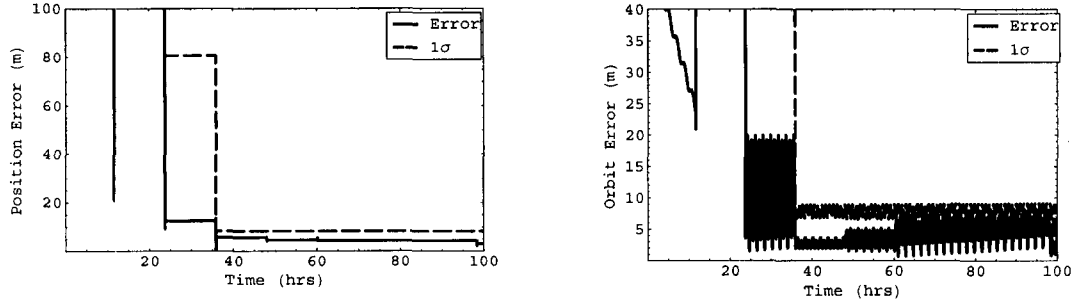


**Figure 3:** Filter errors and uncertainties for the surface asset position (left) and MRO (right) for Case 1 – no clock errors or estimation.

solution for the node shows that there is no improvement in its uncertainty from its initial value, that is  $\sigma_{\Omega}(t) = \sigma_{\Omega}(t_0) = 0.00014^\circ$ . Furthermore, because  $y^{sa}$  is correlated to  $\Omega$  their uncertainties can be related as follows,

$$\sigma_{y^{sa}} \cong R_m \sigma_{\Omega} \cong 8\text{m}. \quad (22)$$

Hence, when  $\sigma_{y^{sa}}$  reaches 8 m it cannot decrease past the level indicated by the above equation. This suggests that a single link of in-situ 2-Way Doppler data is unable to observe the orbiter ascending node, additional data (and geometry) is required. This result occurs for additional cases involving MTO, or with the lander located at higher latitude. These results suggest that this is a generic characteristic.

## Case 2

This case is similar to Case 1, but now there are clock bias, drift, and noise errors present, and the simulation runs for 200 hrs. However, the filter still does not estimate for the clock components. This case is useful for examining how clock errors alias into the solution for the surface asset and the orbiter. The specific levels of the clock errors are as follows,

1. Bias error  $\delta b = 50$  msec (i.e.,  $\bar{b} = 0$ ),
2. Drift error  $\delta d = -1 \times 10^{-7}$  (i.e.,  $\bar{d} = -5 \times 10^{-8}$ )
3. Clock query noise of 60 nsec.

From the discussion on Mars timekeeping these are large values relative to the expected 10 msec bias error, and  $1 \times 10^{-10}$  drift error. Simulation results are shown in Figure 4 (located after the references). As expected, the clock error and uncertainty grows without bound (see the bottom-center plot). The surface asset position error exhibits a very slow divergence from truth. Indeed, at the end of 200 hrs the surface asset position error (top-left plot) is  $\sim 30$  m, a 3-sigma result, indicating that surface asset positioning is relatively insensitive to clock error. This same observation is not true for the orbit error. Examination of the top-right plot shows that the error is growing secularly and is 41

times larger than the associated uncertainty. The filter has ‘aliased’ the clock error into the orbit solution more so than into the surface asset solution. The reasons for this will be made clearer in a later case.

### Case 3

This is the same as Case 2, however, the filter now estimates for the clock bias and drift terms, along with the surface asset and orbiter positions. The results, shown in Figure 5, indicate that there is no aliasing of the clock error into the orbiter or surface asset solution. The solutions are consistent with their uncertainties; however the uncertainty levels remain large. The surface asset uncertainty is  $\sim 25$  m, the orbiter’s is  $\sim 350$  m, and the clock’s settles to near 100 msec. The filter solutions, however, perform much better than the uncertainties indicate; indeed the surface asset error is less than 10 m.

### Case 4

This case examines the “nominal” case where the clock errors have been resolved to levels of 1 msec for the bias error and  $5 \times 10^{-10}$  for the drift rate error. These levels are expected over an extended period of time correlation data processing, and prior surface asset positioning processing. The filter estimates for surface asset, clock, and orbiter. Like Case 1, the process noise  $Q(t)$  has been set to very small levels, about  $1/100000^{\text{th}}$  of the actual errors. The results of this case are shown in Figure 6. The solutions are well behaved and produce errors consistent with the statistics. The surface asset position uncertainty reaches 8 m and levels out for the same reason it did in Case 1 – the  $y^{sa}/\Omega$  correlation coupled with the unobservability of  $\Omega$ . The results show another correlation (alluded to in Case 2) between the orbiter and the clock. In fact, the clock bias is fully correlated to the orbiter mean anomaly ( $P_{b,M_o} / (\sigma_b \sigma_{M_o}) = -0.99$ ), and as before the correlation yields floor uncertainty levels for the orbiter and clock error. Indeed, unlike Case 3 where there was some improvement in the clock uncertainty (falling 500 msec to 100 msec), here there is none. This correlation leads to the following relationship,

$$\sigma_{\text{orbiter}} \sim a\sigma_{M_o} \sim a n \sigma_{\text{ECLK}} \quad (23)$$

which, upon substituting the steady state clock uncertainty  $\sigma_{\text{ECLK}} = 10\text{msec}$  seen in the clock error in Figure 6 into Eq. (23), yields a 34 m error that matches the steady orbiter error  $\sigma_{\text{orbiter}}$  seen in the figure. So a natural question to ask is will the addition of DTE data eliminate or, at least, decrease these correlations? The answer to this question is addressed in the next case.

### Case 5

This case adds DTE Doppler between MRO and DSS 45. Additionally, the process noise is increased from Case 4, otherwise all other characteristics of this simulation are the same as in Case 4. This case represents a nominal operating scenario where both in-

situ and DTE data are available, and some knowledge exists about the ECLK behavior. Figure 7 illustrates that the filter is able solve for the surface asset position with errors that are less than 10 m. The associated uncertainties reach a steady state value near 10 m. The orbit error is in the 10 m range, which is consistent with the current operational experience at Mars.<sup>7</sup> The clock error and uncertainties are in the 2 – 3 msec regime, and the data geometry is sufficient to observe and decrease the clock drift rate uncertainties. Finally, the correlations that existed with the in-situ data only cases have been eliminated. Additional cases (not shown) reach this same level of performance in the presence of very large initial clock errors. This case provides strong evidence that surface asset positioning will be able to achieve 10 m accuracy in the presence of in-situ time tag errors.

### **Case 6**

This final case is the same as Case 5, except that MRO has been replaced by MTO. MTO is in a much higher orbit which means pass lengths are longer, but, since MTO has a slower velocity, the Doppler signature is smaller relative to MTO. The strength of Doppler data over a given period of time is, to first order, dependent on the magnitude of the mean motion, which for MTO is less than MRO.<sup>8</sup> Figure 8 shows the results for this case. The actual filter solutions are commensurate with MRO, except for the drift rate. The associated uncertainties are higher (i.e., the surface asset position uncertainty ~ 20 m), which is a consequence of MTO's smaller Doppler signature relative to MRO.

### **CONCLUSIONS**

This study has described the current design being pursued by the Mars Network for maintaining time at Mars. The resulting system is anticipated to yield clock uncertainties at ~ 10 msec level. The central question addressed in the paper, "Is this error sufficiently small for surface asset positioning to achieve 10 m accuracies?" The results for cases with only in-situ data clearly illustrate that surface asset positioning is relatively insensitive to Doppler time tag errors. However, significant correlations exist between the asset's y-position and the orbiter's ascending node and between the clock bias and the orbiter's initial mean anomaly. The addition of DTE Doppler data to the orbiter removes these correlations and yields a robust positioning system capable of meeting the 10 m requirement in the presence of significant in-situ time tag errors.

### **ACKNOWLEDGEMENTS**

This work was carried out at the Jet Propulsion Laboratory, California Institute of Technology, under contract with the National Aeronautics and Space Administration.

### **REFERENCES**

1. Bell, D. J., Cesarone, R., Ely, T. A., Edwards, C., Townes, S. "Mars Network: A Mars Orbiting Communications & Navigation Satellite Constellation." Paper #252, 2000 IEEE Aerospace Conference, Big Sky, MT, March 18-25, 2000.

2. Hastrup, R. C., Bell, D. J., Cesarone, R. J., Edwards, C. D., Ely, T. A., Guinn, J. R., Rosell, S. N., Srinivasan, J. M., Townes, S. A., "Mars Network for Enabling Low-Cost Missions." Paper # IAA-L-0509, Fourth IAA International Conference on Low-Cost Planetary Missions, The Johns Hopkins University, Applied Physics Laboratory, Laurel, MD, May 2-5, 2000.
3. Edward, C. D., Adams, J. T., Bell, D. J., Cesarone, R., Depaula, R., Durning, J. F., Ely, T. A., Leung, R. Y., McGraw, C. A., Rosell, S. N., "Strategies for Telecommunications and Navigation in Support of Mars Exploration." Paper No. IAF-00-Q.3.05, 51<sup>st</sup> International Astronautical Congress, Rio de Janeiro, Brazil, Oct 2 – 6, 2000.
4. Moyer, T. D., *Formulation for Observed and Computed Values of Deep Space Network Data Types for Navigation*. Deep-Space Communications and Navigation Series, John Wiley & Sons, 2003.
5. Ely, T. A., "Electra 2-Way Doppler Measurement Model including Error Budget: Revision 2." Electra-IOM-03-018 (internal JPL document), January 15, 2003.
6. Bierman, G. J., *Factorization Methods for Discrete Sequential Estimation. Mathematics in Science and Engineering*. Vol. 128, Academic Press, 1977.
7. Demacak, S., Graat, E., Esposito P. B., Baird, D. T., "Mars Global Surveyor Mapping Orbit Determination." Paper No. AAS 01-100, AAS/AIAA Space Flight Mechanics Meeting, Santa Barbara, California, Feb. 11 – 15, 2001.
8. Ely, T. A., Guinn, J., "Mars Approach Navigation using Mars Network Doppler Data." Paper No. AIAA 2002-4816, AIAA/AAS Astrodynamics Specialist Conference, Monterey, CA, August 5 – 8, 2002.

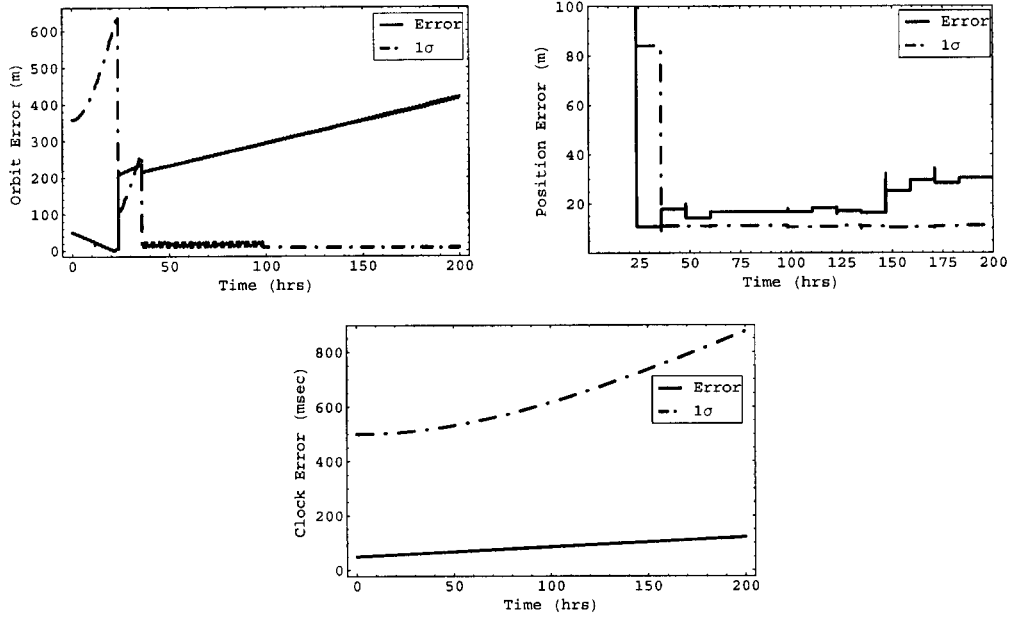


**Figure 4:** Filter errors and uncertainties for the surface asset position (top-left) and MRO (top-right), ELCK (bottom-center) for Case 2 – large clock errors and no estimation.

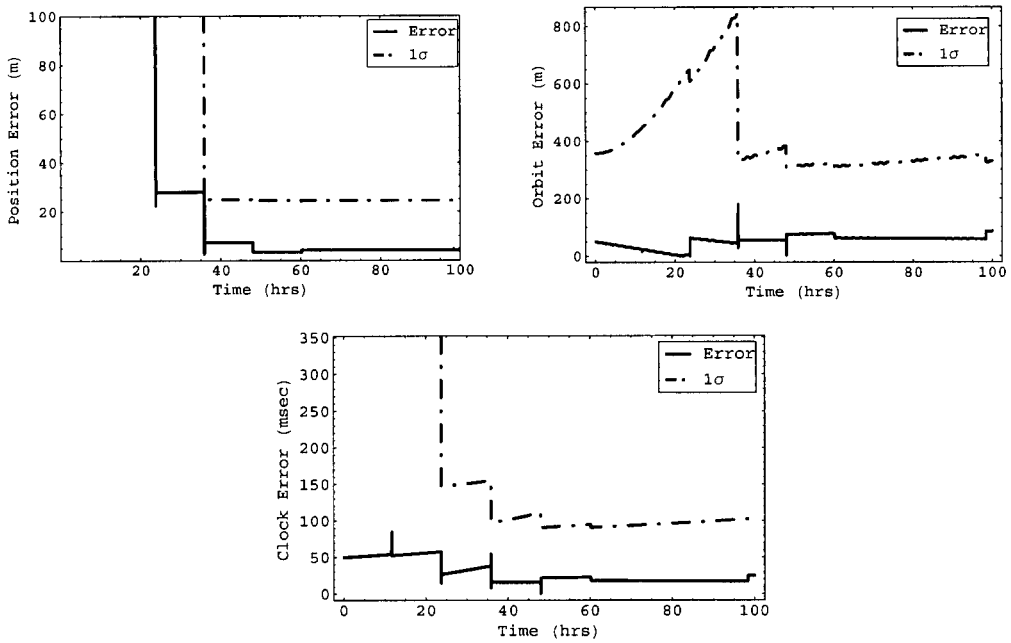


**Figure 5:** Filter errors and uncertainties for the surface asset position (top-left) and MRO (top-right), ELCK (bottom-center) for Case 3 – large clock errors and clock estimation.

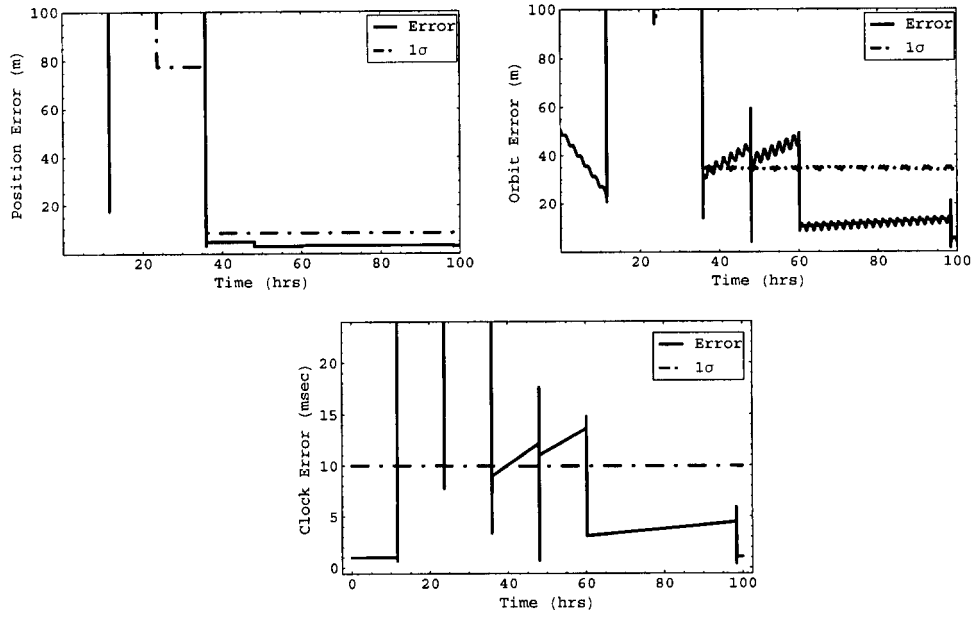


**Figure 6:** Filter errors and uncertainties for the surface asset position (top-left) and MRO (top-right), ELCK (bottom-center) for Case 4 – nominal clock error & estimation, small process noise.

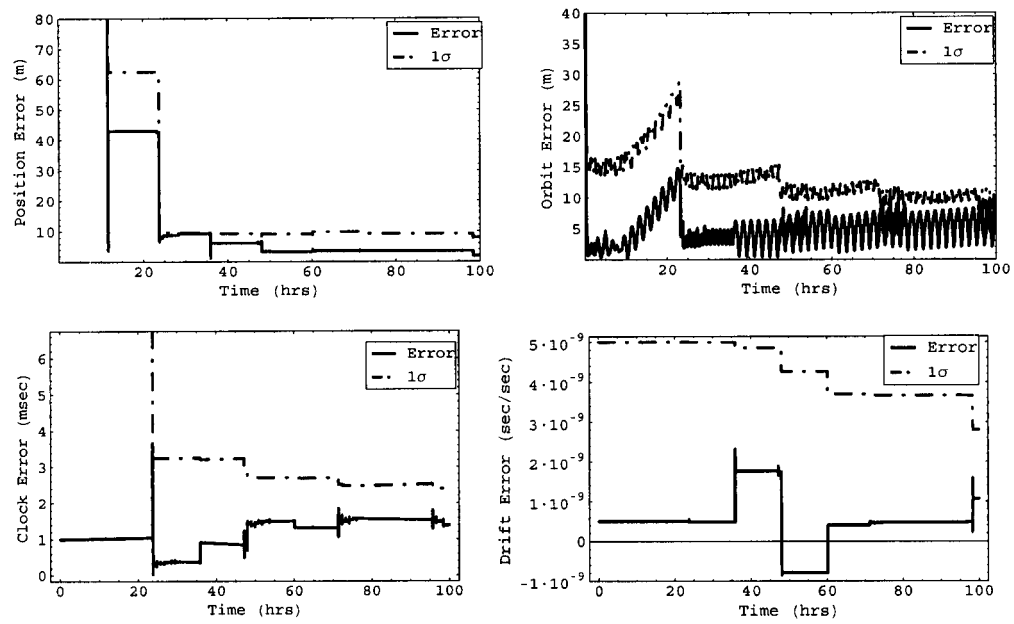


**Figure 7:** Filter errors and uncertainties for the surface asset position (top-left) and MRO (top-right), ELCK (bottom-center) for Case 5 – nominal case with in-situ and DTE data.

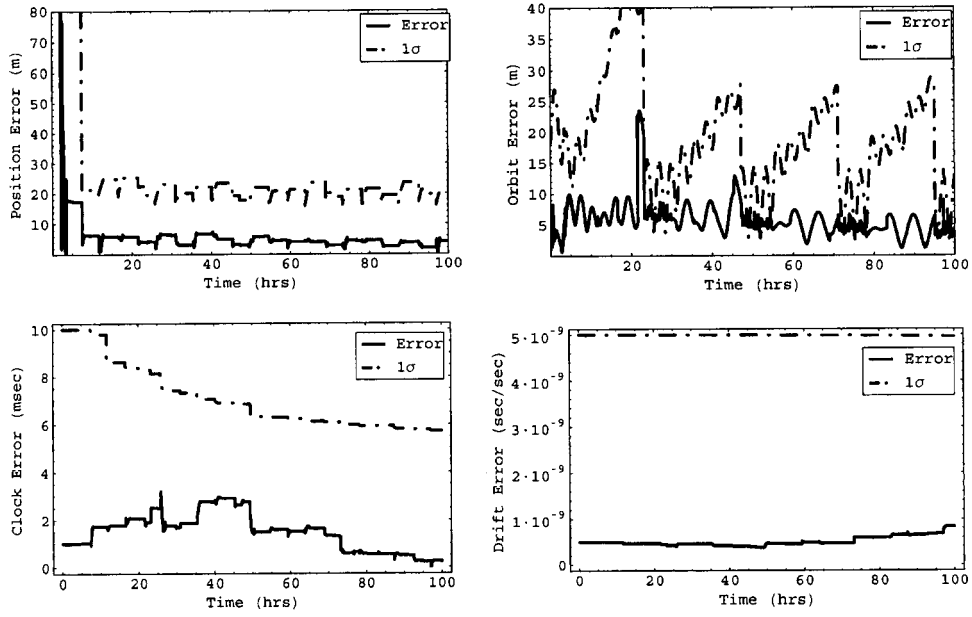


**Figure 8:** Filter errors and uncertainties for the surface asset position (top-left) and MRO (top-right), ELCK (bottom-center) for Case 5 – nominal case with in-situ and DTE data.